ARRIVAL TIME PICKING OF MICROSEISMIC DATA BY USING SPE ALGORITHM

XINTONG DONG [1], HONG JIANG [1], YUE LI [1] and BAOJUN YANG [2]

[1] *Jilin University, Department of Information Engineering, Changchun Jilin 130000, P.R. China. 18186829038@163.com; jiangh@jlu.edu.cn; liyue@jlu.edu.cn*
[2] *Jilin University, Department of GeoExploration Science and Technology, Changchun Jilin 130000, P.R. China.*

(Received August 30, 2018; revised version accepted August 10, 2019)

ABSTRACT

Dong, X.T., Jiang, H., Li. Y. and Yang, B.J., 2019. Arrival time picking of microseismic data by using SPE algorithm. *Journal of Seismic Exploration*, 28: 475-494.

The accuracy of the arrival time picking has deep influence on hypocenter location which is the core part of microseismic exploration, so arrival time picking plays a significant role in microseismic date processing. However, at this stage, the arrival picking of microseismic signals with low signal-to-noise ratios (SNR) are problematic because these valid signals are usually obscured by random noise, so it is difficult to obtain the arrival time of microseismic signal accurately by the conventional methods, especially the horizontal components in microsiesmic signals. In order to solve this technical issue, the valid signals in microseismic data is highlighted by the multi-scale and multi-direction features of Shearlet transform, and because of the vibration track's difference between the valid signals and noise, the polarization analysis is applied to process the Shearlet coefficients. Also, through the introduction of entropy and the proposal of weight factor, three-dimensional (3D) weighted entropy algorithm is constructed, so as to achieve the purpose of processing the three components together. Several synthetic and field data examples with different kinds of noise demonstrate the effectiveness and robustness of the Shearlet transform-polarization analysis-3D weighted entropy (SPE) algorithm in arrival time picking of microseismic data.

KEY WORDS: arrival time picking, microseismic data, random noise, Shearlet transform, polarization analysis, weighted entropy ratio.

0963-0651/19/$5.00

INTRODUCTION

Arrival time picking for microseismic signals is a significant step in both microseismic events detection and hypocentral location (Warpinski, 2009). However, due to the low SNR (Rodriguez et al., 2011), the arrival time of microseismic signals can not be accurately picked through the conventional methods, and the manual time picking method is tedious and time-consuming. Therefore, an accurate automatic time picking method for microseismic data is urgently needed (Saragiotis et al., 2002).

At the present stage, most of the commonly used methods for microseismic arrival time picking come from the algorithms for conventional seismic signals, such as the akaike information criterion (AIC), short time window average and long time window average (STA/LTA) algorithm and so on (Leonard and Kennett, 1999). The STA/LTA algorithm was proposed by Stevenson (1976). In this algorithm, the absolute value, the energy or the envelope of the microseismic event are often selected as the characteristic function (Allen, 1978). The arrival time is detected when the ratio of characteristic function is larger than a preset threshold (Allen, 1982). The drawback of this algorithm is that the selection of windows' length needs careful consideration and the false picking often appears when SNR is low. The AIC method is based on an autoregressive modeling. The point of the minimum AIC value is regarded as the arrival time, but when dealing with actual microseismic data with low SNRs, several local minimal AIC values will appear which may lead to the false time picking.

The Shearlet transform proposed by Labate and Guo (2007) is a combination of wavelet theory and geometric multi-scale analysis (Houska and William, 2007). The Shearlet transform has obvious advantages in sparse representation characteristics and the operation rate (Zhao et al., 2016), so this transform must be suitable for microseismic data processing.

In the conventional methods, the arrival time of the microseismic signals' three components is picked by single-trace processing (Tetsuo and Kitagawa, 1991), so the conventional methods do not take the correlation of three components into consideration. Moreover, the false pickings often appear in horizontal components, and the picking results of three components are always different, which is not consistent with the fact (Allen, 1978). In SPE algorithm, we propose a new weight factor which can reflect the distribution of the signals' amplitude and frequency, and introduce the entropy to construct the 3D weighted entropy algorithm. The 3D weighted entropy algorithm is combined with polarization analysis and Shearlet transform, so as to effect of processing three components together. In this way, correlation of three components is taken into account, which is conducive to the arrival time picking of microseismic data. The specific process of SPE algorithm is shown in Fig 1. In comparison with the conventional methods, whether synthetic or field microseismic data demonstrate the superior performance of SPE algorithm on accuracy and reliability.

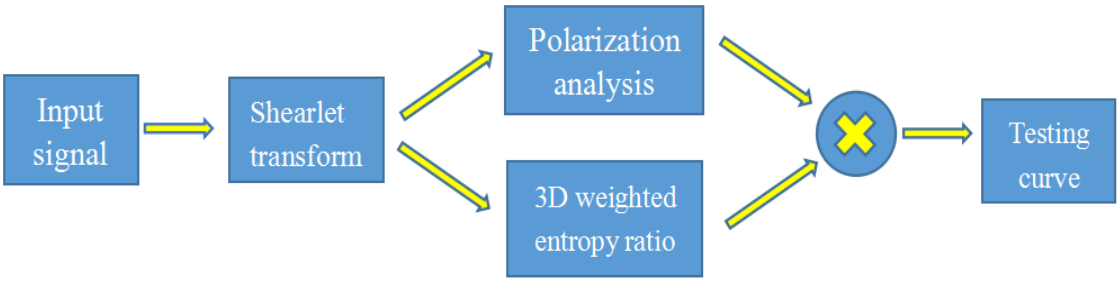

Fig. 1. The specific progress of the SPE algorithm.

THE SHEARLET TRANSFORM

Shearlet transform is a new multi-scale geometric analysis method (Kutyniok and Labate, 2007). The Shearlet transform has excellent characteristics in multi-scale, multi-direction and anisotropy. Compared with other transforms, such as Curvelet transform and wavelet transform, Shearlet transform can provide a precise and simple metrical characterization for signal analysis and it also has obvious advantages in frequency separation (Guo and Labate, 2007). In this part, the basic theories of Shearlet transform are introduced briefly. The expression of the Shearlet is as follows

$$\left\{\psi_{ast}(x)=\left|\det M_{as}\right|^{-\frac{1}{2}}\psi\left(M_{as}^{-1}(x-t)\right): a\in R^{+}, s\in R, t\in R^{2}\right\} \quad (1)$$

In eq. (1), parameters a, s, t represents the scale, location, orientation, respectively. R, R^{+}, R^{2} indicate the sets of real numbers, positive real numbers, and two dimensional real numbers, respectively. M_{as} is the composition of the anisotropic dilation matrix $A_a=\begin{pmatrix} a & 0 \\ 0 & \sqrt{a} \end{pmatrix}$ and the shear matrix $S_S=\begin{pmatrix} 1 & -S \\ 0 & 1 \end{pmatrix}$. ψ is the Shearlet generating function which should satisfy appropriate admissibility conditions. For any $\xi=(\xi_1,\xi_2)\in\hat{R}^2$, $\xi_1\neq 0$, ψ should satisfy the following equation:

$$\hat{\psi}(\xi)=\hat{\psi}(\xi_1,\xi_2)=\hat{\psi}_1(\xi_1,\xi_2)\hat{\psi}_2(\frac{\xi_2}{\xi_1}) \quad , \tag{2}$$

where $\hat{\psi}$ represents the Fourier transform of ψ. ψ_1 indicates the continuous wavelet function and ψ_2 is the bump function, with the support $\hat{\psi}_1,\hat{\psi}_2\in C^{\infty}(\hat{R})$, $\mathrm{supp}\hat{\psi}_1\subset[-\frac{1}{2},-\frac{1}{16}]\cup[\frac{1}{16},\frac{1}{2}]$, $\mathrm{supp}\hat{\psi}_2\in[-1,1]$, with $\psi_2>0,\|\psi_2\|=1$ on $[-1,1]$. So the support condition of $\hat{\psi}_{ast}$ in frequency domain is as follows:

$$\mathrm{supp}\hat{\psi}_{a,s,t}\subset\{(\xi_1,\xi_2):\xi_1\in[-\frac{2}{a},-\frac{1}{2a}]\cup[\frac{1}{2a},\frac{2}{a}],|s+\frac{\xi_2}{\xi_1}|\le a^{\frac{1}{2}}\} \quad . \tag{3}$$

Eq. (3) shows that, in the case of different scales, the frequency domain support of $\hat{\psi}_{a,s,t}$ is symmetric about origin. When the Shear parameters is changed, the area of the supporting region varies with rotation, and the supporting area gradually narrows into a strip as a→0. In particular cases, the frequency domain support of $\hat{\psi}_{a.s.t}$ as shown in Fig. 2.

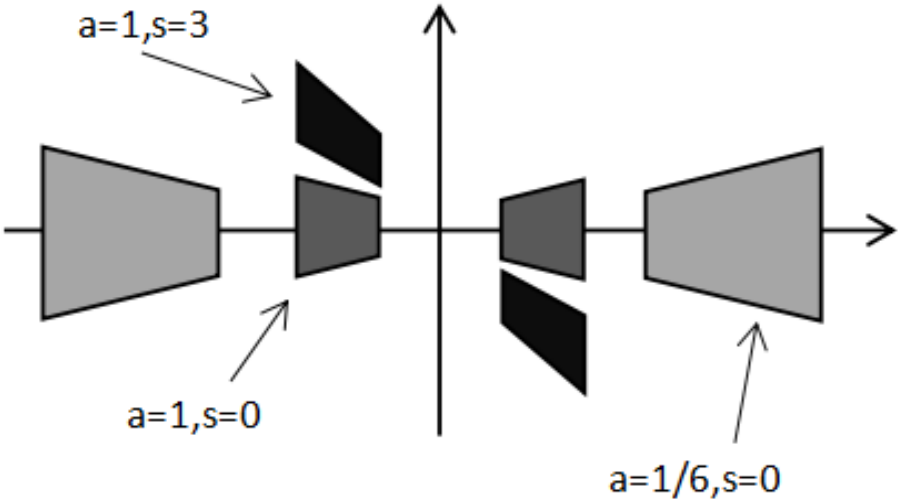

Fig. 2. Frequency domain support of the Shearlets for different values of a and s.

The continuous Shearlet transform is defined as the function (Yi et al., 2009:

$$SH_{\psi}(f) = \langle f, \psi_{ast} \rangle \quad , \tag{4}$$

where $\langle . \rangle$ defines inner product, SH_{ψ} is the Shearlet transform and f stands for input signal.

For the convenience of computer calculation, the discrete Shearlets is introduced by Kutyniok and Labate (2007) as (Kutyniok and Lim, 2011):

$$\left\{ \psi_{jkm}(x) = \left| \det A_4 \right|^{-j/2} \psi\left(S_1^{-k} A_4^{-j} x - m \right) : j,k \in \mathbf{Z}, m \in \mathbf{Z}^2 \right\} \quad . \tag{5}$$

The discrete Shearlets samples the parameters *a,s* and *t* into a discrete set, the scales parameter $a_j = 4^j$, the location parameter $t_{jkm} = s_{k2^j} A_{4^j} m$ and the orientation parameter $s_{jk} = k2^j$ (where $a > 0$, $s \in \mathbf{R}$, $t \in \mathbf{R}^2$, and $j,k \in \mathbf{Z}$ $m \in \mathbf{Z}^2$).

THE SPE ALGORITHM

The SPE algorithm is mainly based on the Shearlet transform, the polarization analysis and the 3D weighted entropy ratio algorithm. The valid signals in microseismic data are highlighted in Shearlet domain. Due to the high-frequency feature of effective signals, the higher frequency scales contain more information of the effective signals. By making full use of Shearlet transform's correlation in adjacent scales, two groups of Shearlet coefficients in a same direction are selected at the highest-frequency scale and the second highest-frequency scale, we can obtain the final coefficients through the two groups of Shearlet coefficients.

In order to verify the effectiveness of Shearlet transform, the Ricker wavelet and white gaussion noise (WGN) are used to simulate the actual three components of microseismic signals. The expression of Ricker wavelet is as follows:

$$X(t) = \left(1 - 2\pi^2 f_0^{\,2} t^2\right) \exp\left(-\pi^2 f_0^{\,2} t^2\right) \quad , \tag{6}$$

where f_0,t respectively represent central frequency and time. The WGN is added into Ricker wavelet. The SNR, sampling frequency and central frequency of the synthetic data is -7 dB, 1000 Hz, 300 Hz, respectively. After the Shearlet transform, we can obtain Shearlet coefficients of different scales and different directions (there are five scales in the transform and every scale has six directions). By calculating the power of final Shearlet coefficients in different directions, the power of fifth direction is the biggest. Since the uniform energy distribution of white noise in six directions, the fifth direction contains more components of valid signals. So the fifth direction is selected as the experimental subject.

In Fig. 3(b), trace 1, 2, 3 are the X, Y, Z components, respectively. In Fig. 3(b), the valid signals are almost obscured by the noise, especially in X,Y components. Compared with the noisy signal in Fig. 3(b), the final Shearlet coefficients in Fig. 3(c) include more effective information of valid signals. So the Shearlet transform can highlight the valid signals effectively.

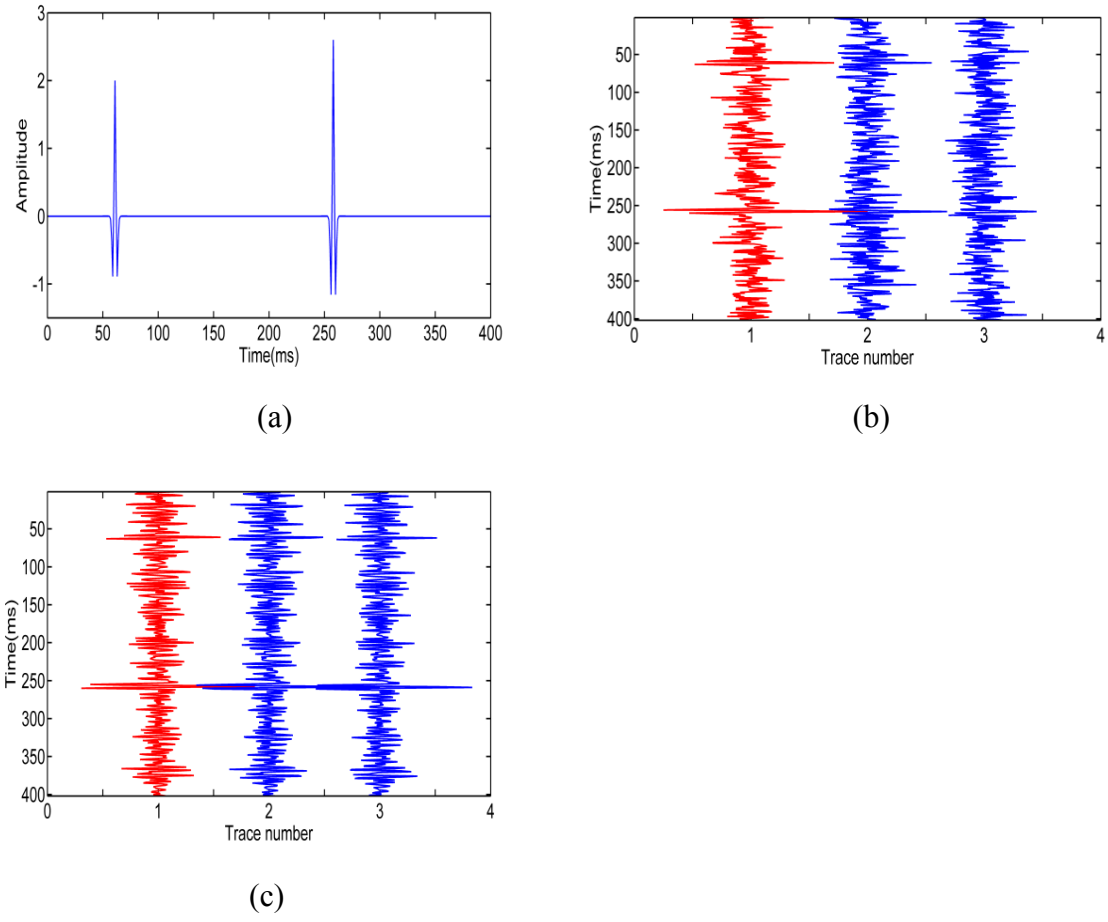

Fig. 3. (a) The Ricker wavelet without noises. (b) The synthetic three components of microseismic signals with WGN (SNR = -7 dB). (c) The final Shearlet coefficients.

Polarization analysis

The polarization analysis method proposed by Deflandre and Dubesset (1992) is mainly based on the vibration track. Because there are obvious differences between the noise and the effective signal in the vibration track, the polarization analysis method can be applied to the processing of microseismic data. In this method, the arrival time is extracted by calculating the polarization degree. In SPE algorithm, the microseismic signals are replaced by the final Shearlet coefficients, which can effectively rise the accuracy of arrival time picking. The sliding time windows are introduced to obtain the data of partial final Shearlet coefficients, and then we establish the convariance matrix whose expression is as follows:

$$M_i = \begin{bmatrix} E\left[(X_i - E[X_i])^2\right] & E[(X_i - E[X_i])(Y_i - E[Y_i])] & E[(X_i - E[X_i])(Z_i - E[Z_i])] \\ E[(Y_i - E[Y_i])(X_i - E[X_i])] & E\left[(Y_i - E[Y_i])^2\right] & E[(Y_i - E[Y_i])(Z_i - E[Z_i])] \\ E[(Z_i - E[Z_i])(X_i - E[X_i])] & E[(Z_i - E[Z_i])(Y_i - E[Y_i])] & E\left[(Z_i - E[Z_i])^2\right] \end{bmatrix} \tag{7}$$

E expresses the expectation of the final Shearlet coefficients. i stands for the i-th sampling point. X_i, Y_i, Z_i stands for the X, Y, Z components of the final Shearlet coefficients, respectively. In eq. (8), the final Shearlet coefficients of microseismic three components are processed together rather than single trace processing. We solve the three eigenvalues of convariance matrix M_i. The polarization analysis curve (P curve) is constructed by the eigenvalues. The expression of the P curve is as follows:

$$P_i = \frac{\left(\lambda_i^1 - \lambda_i^2\right)^2 + \left(\lambda_i^1 - \lambda_i^3\right)^2 + \left(\lambda_i^2 - \lambda_i^3\right)^2}{2\left(\lambda_i^1 + \lambda_i^2 + \lambda_i^3\right)^2} \quad . \tag{8}$$

$\lambda^1, \lambda^2, \lambda^3$ respectively represent three different eigenvalues of convariance matrix M_i. The scope of the p_i is 0~1. When $P = 1$, the signal is linearly polarized. When $P = 0$, the signal is circular polarized (such as random noise. Compared with the random noises, the p of the valid signal is much larger, so the valid signals can be highlighted in P curves. In Fig. 4, the P curves are shown respectively with different SNRs. Whether SNR = -7 dB or -10 dB, the valid signals are highlighted in the P curves.

3D Weighted entropy ratio

The STA/LTA algorithm is widely used in arrival time picking of seismic signals. The expression of conventional STA/LTA algorithm is as follows:

$$R_i = \frac{STA_i}{LTA_i} = \frac{\left(CF_i - CF_{i-N_2}\right)/N_2 + STA_{i-1}}{\left(CF_i - CF_{i-N_1}\right)/N_1 + LTA_{i-1}} \quad , \tag{9}$$

N_1 is the length of long sliding window, N_2 is the length of short sliding window, CF_i is the characteristic function. In conventional STA/LTA algorithm, the parameters of signal, such as power, amplitude, variance and so on, are regarded as the characteristic function. However, when dealing with the microseismic data with lower SNR, the conventional characteristic function has insufficient sensitivity to effective signals, so the conventional STA/LTA algorithm can not meet the requirement of arrival time picking of the microseismic signals.

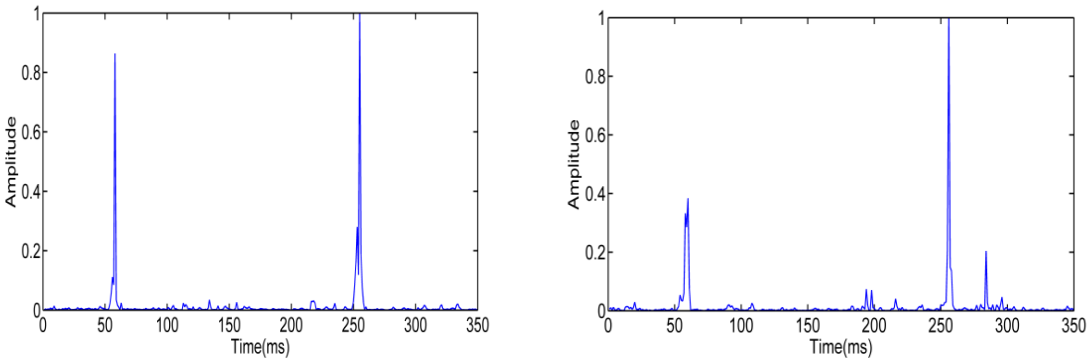

(a) (b)

Fig. 4. (a) The *P* curve when SNR = -7 dB. (b) The *P* curve when SNR = -10 dB.

In order to rise the sensitivity to the valid signals, the weight factor is proposed and the entropy is introduced into arrival time picking. The expression of weight factor is as follows:

$$W = \sum_{i=1}^{N} |x_i| \Big/ \sum_{i=1}^{N} |x_i'| \quad . \tag{10}$$

x_i is the final Shearlet coefficients, x_i' is the derivative of final Shearlet coefficients, and N represents the length of windows. According to the change of frequency and energy when arrival time comes, the function P is constructed. The expression of function P is as follow:

$$P = W|x_i - x_{i-1}|^2 + x_i^2 \quad , \tag{11}$$

where W represents the weight factor in eq. (10). In informatics, entropy represents the degree of chaos, the entropy of window will largely increase when arrival time comes, so this statistic is suitable for microseismic data processing. We calculate the function P value of each point in windows. The expression of weighted entropy WE is as follow：

$$WE = -\sum_{i=1}^{N} \frac{P_i}{SUMP} \ln \frac{p_i}{SUMP} \tag{12}$$

$$SUMP = \sum_{i=1}^{N} P_i \quad . \tag{13}$$

The weighted entropy WE is regarded as the new characteristic function.

In conventional STA/LTA algorithm, the three components of microseismic signal are processed respectively. In low SNRs, the picking results of X, Y, Z components in one group are always different, which is not in accordance with the facts. Also, the picking results of X,Y components are always wrong because the valid signal's energy in X,Y components is weak. In order to solve this drawback, the ratios of the short window weighted entropy and long window weighted entropy in three components are calculated respectively. The entropy curve (E curve) is built by the three ratios. The expression of the E curve is as follow:

$$E(i) = \left(WE_x^2 + WE_y^2 + WE_Z^2\right)^{\frac{1}{2}} \quad . \tag{14}$$

In eq. (14), WE_x, WE_y, WE_Z represent the weighted entropy ratios of final Shearlet coefficients in X,Y,Z components, respectively. In Fig. 5, the E curves are shown respectively with different SNRs. From Fig. 5, we can draw a conclusion that the weighted entropy ratio curve can availably highlight the valid signals when the SNR is as low as -10 dB.

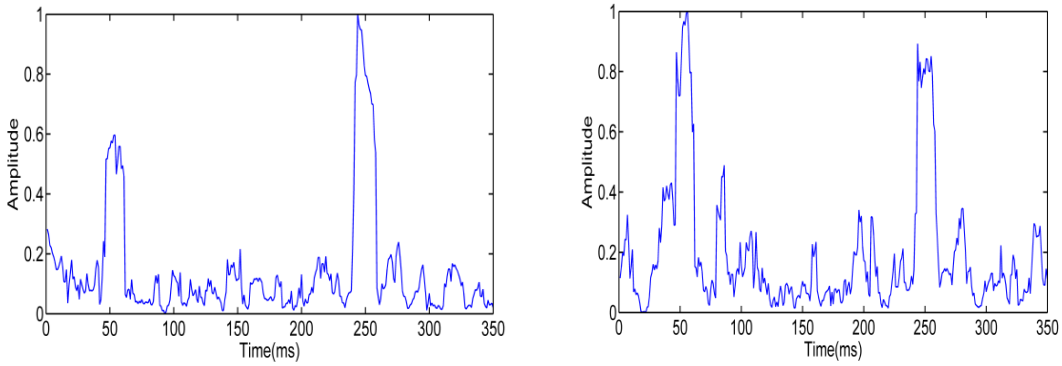

(a) (b)

Fig. 5 (a) The E curve when SNR = -7dB. (b) The E curve when SNR = -10dB.

The *E* curve and the *P* curve are multiplied to obtain the testing curve (*T* curve). The Maximum point of the first take-off in the *T* curve is regarded as the arrival time. In Fig. 6, the *T* curves with different SNRs are shown. It is obvious that the valid signals are effectively highlighted in *T* curves. So the SPE algorithm can pick the arrival time precisely.

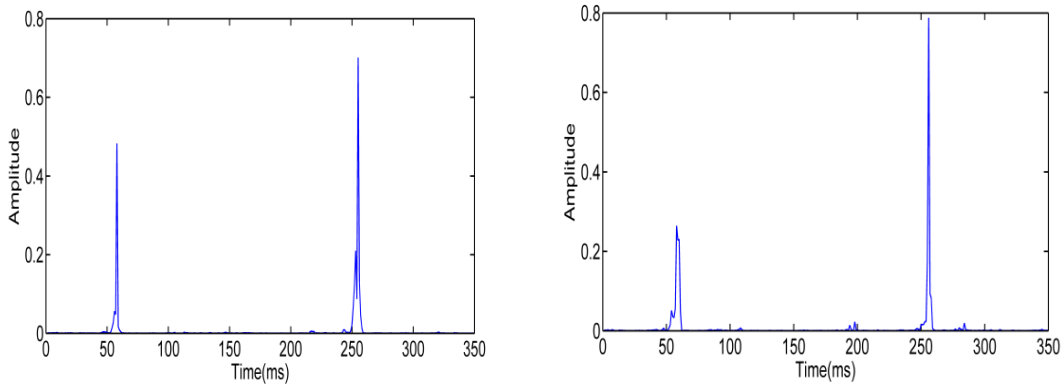

(a) (b)

Fig. 6. (a) The T curve when SNR = -7 dB. (b) The T curve when SNR = -10 dB.

Implementation of the SPE algorithm

(1) By converting the microseismic signals into Shearlet domain, we can obtain coefficients of different scales and directions(there are five scales in the transform and every scale contains six directions)
(2) At the highest-frequency scale and the second high-frequency scale, we select two groups of Shearlet coefficients in most energetic direction, and the final coefficients are obtained through the two selected groups of Shearlet coefficients' correlation
(3) By making full use of sliding windows and three components' correlation, the convariance matrix of final Shearlet coefficients is constructed, and though calculating the eigenvalues of convariance matrix, the P curve is established.
(4) We calculate the weighted entropy ratios of final Shearlet coefficients in X,Y,Z components, respectively, and the E curve is obtained through the three ratios.
(5) The *E* curve and the *P* curve are multiplied to obtain the *T* curve. The Maximum point of the first take-off in *T* curve is regarded as the arrival time.

TESTS WITH SYNTHETIC MICROSEISMIC DATA

Feasibility

In order to test the feasibility of SPE algorithm in different SNRs, we generate a Ricker wavelet with dominant frequency of 300 Hz and sample frequency of 1000 Hz. We add WGN and real noise to this Ricker wavelet, and make the SNR = -5 dB, -7 dB, -10 dB, respectively. In this paper, we consider time picking is accurate when the error is within 0.003 s (within three sampling points).

We verify the reliability of SPE algorithm by repeated experiments. In Table I and Table II, the results of SPE algorithm are listed. On the whole, no matter the type of the noise, the accuracy of SPE algorithm is very high. In WGN tests, the accuracy rate of SPE algorithm is 99.5%, 99%, 89.3% when SNR = -5dB, -7dB, -10dB, respectively. In real noises tests, the accuracy rate of SPE algorithm is 99.2%, 98.3%, 90.3% when SNR = -5 dB, -7 dB, -10 dB, respectively. Obviously, the high accuracy of SPE algorithm can certainly meet the requirement of microseismic data processing.

Table I. Time picking results of SPE algorithm in WGN tests.

The WGN tests						
SNR(dB)	numbers of signals	accurate picking	inaccurate picking	Signals picking within 0.002s	Signals picking within 0.001s	Signals picking without errors
-5	1000	995	5	966	912	740
-7	1000	990	10	943	864	632
-10	1000	893	107	760	656	520

Table II. Time picking results of SPE algorithm in real noises tests.

The real noises tests						
SNR(dB)	numbers of signals	accurate picking	inaccurate picking	Signals picking within 0.002s	Signals picking within 0.001s	Signals picking without errors
-5	1000	992	8	977	923	780
-7	1000	983	17	954	890	683
-10	1000	903	97	791	692	561

Advantages

In order further verify the advantages of SPE algorithm,we compare the SPE algorithm with the STA/LTA algorithm and the conventional polarization analysis. In STA/LTA algorithm, the energy of signals is

regarded as the characteristic function. The results of STA/LTA algorithm are shown in Table III and IV. In WGN tests, the accuracy rate of STA/LTA algorithm is 36.4%, 25.4%, 9.4% when SNR = -5dB, -7dB, -10dB, respectively. In real noises tests, the accuracy rate of STA/LTA algorithm is 37.4%, 25.1%, 9.8% when SNR = -5dB, -7dB, -10dB, respectively. The results of the conventional polarization analysis method are shown in Table V and VI. In WGN tests, the accuracy rate of conventional polarization analysis method is 67.6%, 59.9%, 53.4% when SNR = -5dB, -7dB, -10dB, respectively. In real noises tests, the accuracy rate of the conventional polarization analysis method is 67.5%, 58.9%, 52.2% when SNR = -5dB, -7dB, -10dB, respectively. Regardless of the noise type and SNR, the accuracy rate of SPE algorithm is much higher than the conventional methods. The above the statistical data demonstrates that the SPE algorithm has huge advantages over the conventional methods in arrival time picking of microseismic signals.

Table III. Time picking results of STA/LTA algorithm in WGN tests.

The WGN tests						
SNR(dB)	numbers of signals	accurate picking	inaccurate picking	Signals picking within 0.002s	Signals picking within 0.001s	Signals picking without errors
-5	1000	364	636	302	240	86
-7	1000	252	748	216	188	74
-10	1000	94	906	78	58	22

Table IV. Time picking results of STA/LTA algorithm in real noises tests.

The real noises tests						
SNR(dB)	numbers of signals	accurate picking	inaccurate picking	Signals picking within 0.002s	Signals picking within 0.001s	Signals picking without errors
-5	1000	374	626	299	245	92
-7	1000	251	749	210	178	77
-10	1000	98	902	80	64	28

Table V. Time picking results of the conventional polarization analysis in WGN tests.

The WGN tests						
SNR(dB)	numbers of signals	accurate picking	inaccurate picking	Signals picking within 0.002s	Signals picking within 0.001s	Signals picking without errors
-5	1000	676	324	500	294	104
-7	1000	599	401	480	264	96
-10	1000	534	466	364	254	78

Table VI. Time picking results of conventional polarization analysis in real noises tests.

The real noises tests						
SNR(dB)	numbers of signals	accurate picking	inaccurate picking	Signals picking within 0.002s	Signals picking within 0.001s	Signals picking without errors
-5	1000	675	325	504	299	102
-7	1000	589	411	483	262	96
-10	1000	522	478	367	246	74

Error

With aspect to the error, from Table I to Table VI, we can see that the number of signals picking without errors of SPE algorithm is far more than the conventional methods. Also, the numbers of signals picking within 0.001s and 0.002 s of SPE algorithm are also far more than the conventional methods. In order to intuitively show the advantages of SPE algorithm in error controlling, we give the error distribution of the three algorithms when SNR = -7 dB. From the histograms of the error distribution in Fig. 7, taking the real noises tests as example, it is obvious that the main distribution of the SPE algorithm's error is from –0.001s to 0.001s, and the percentage of the picking errors in this range(-0.001s to 0.001s) is 89.0% which is far more than the other two conventional methods. The percentage of picking without error of SPE algorithm is 68.3%, and the percentage of the SPE algorithm's picking errors from -0.002 s to 0.002 s is up to 95.4%. However, the STA/LTA algorithm's picking errors in this range (-0.002s to 0.002s) only make up 21.0% and the conventional polarization analysis method's picking errors in this range (-0.002 s to 0.002 s) only make up 48.3% . So a conclusion can be drawn that whether the picking accuracy or error control, the SPE algorithm is much superior to the other two conventional methods.

Comparison with other algorithms

We generate a synthetic three component microseismic record containing 6 groups of three components with dominant frequency of 300 Hz and sample frequency of 1000 Hz. This record is shown in Fig. 8(a). We add WGN and real noise to this record, and make the SNR = -5 dB, -7 dB, -10 dB, respectively. The vertical components (Z component) are shown in red and the horizontal components (Y,X components) in blue. Fig. 8(a) shows the Ricker wavelet without noise. The noisy record with WGN (SNR = -7 dB) is shown in Fig. 8(b) and the noisy record with WGN (SNR = -10 dB) is shown in Fig. 8(c). Whether SNR = -7 dB or -10 dB, the valid signals are almost submerged by the noise. In Fig. 8(d) and Fig. 8(e), the picking results are shown respectively when SNR is -7 dB and -10 dB and the picking results of SPE algorithm, STA/LTA algorithm and the conventional polarization analysis method are denoted by the symbols in green, black, pink, respectively. When SNR is -7dB, the picking results of SPE algorithm are accurate in all traces, but the wrong traces of STA/LTA algorithm are

1,2,3,8,9,11,12,13,14,15,18 and the wrong traces of the conventional polarization analysis method are 7,8,9,12,18. When SNR is -10dB, the picking results of SPE algorithm are also accurate in all traces, but the picking results of the STA/LTA algorithm are wrong in traces 1,2,6,8,9,10,11,12,15,16,18 and the picking results of the conventional polarization analysis method are wrong in traces 3,7,8,9,12,15,16,17,18.

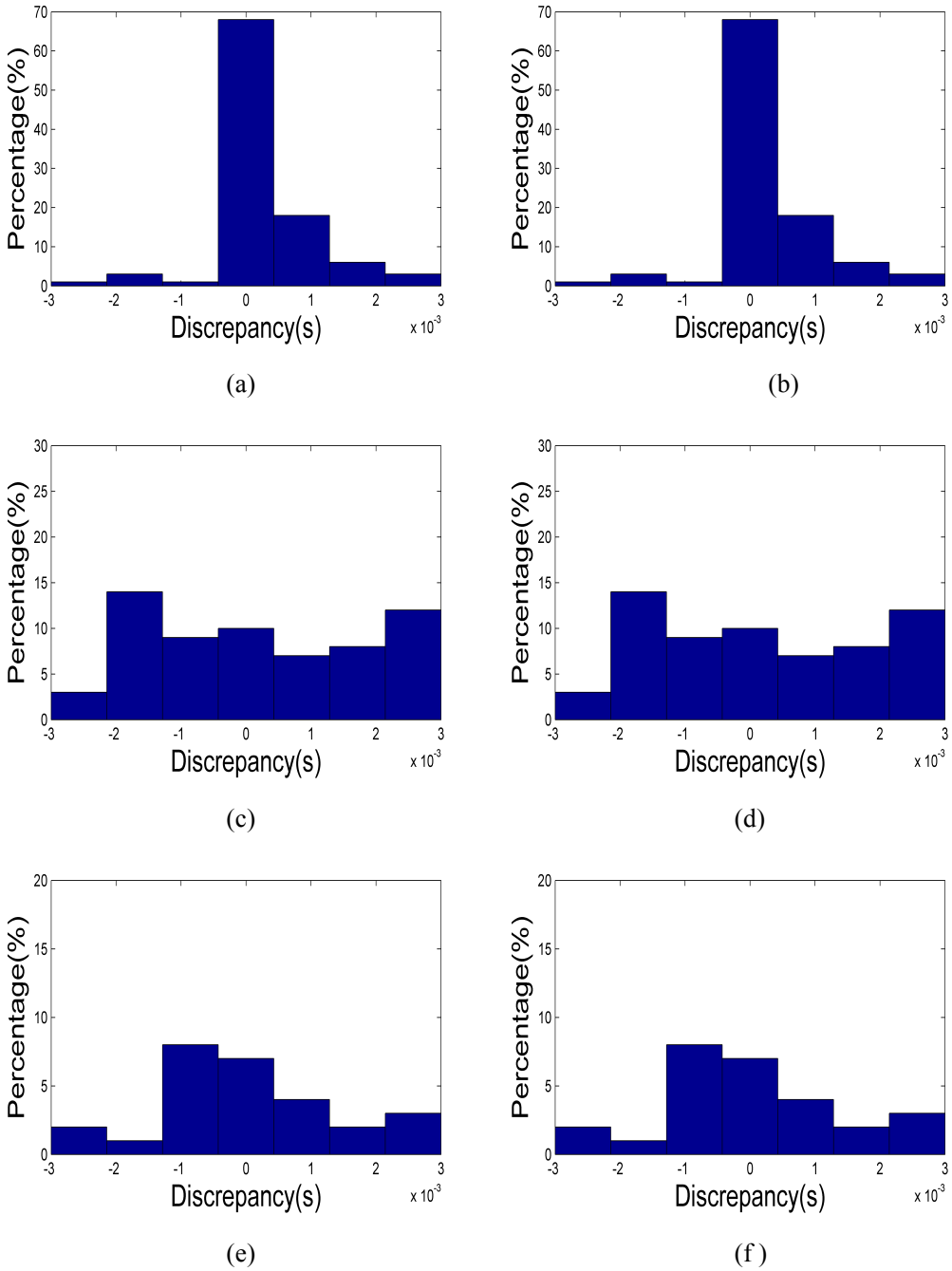

Fig. 7. Histograms of the error distribution. (a) and (b) are error distribution of the SPE algorithm with different noises when SNR = -7 dB, respectively. (c) and (d) are error distribution of the STA/LTA algorithm with different noises when SNR = -7 dB, respectively. (e) and (f) are error distribution of the conventional polarization analysis method with different noises when SNR = -7 dB, respectively.

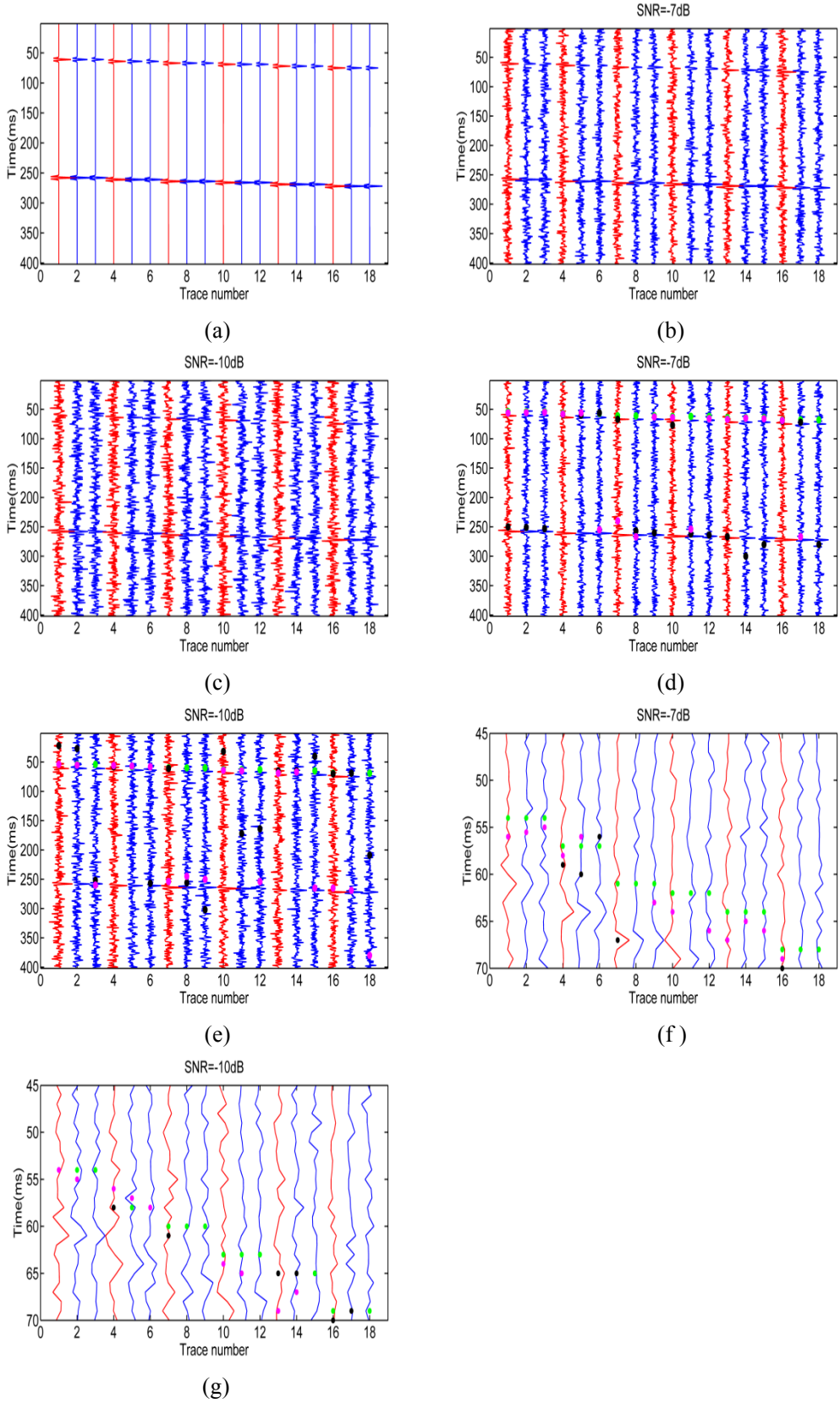

Fig. 8. First arrival times picked by three algorithms with WGN. (a) Ricker wavelet without noise. (b) and (c) are noisy synthetic record with WGN -7 dB and -10 dB, respectively. (d) The automatic picking results of the three algorithms for WGN noisy synthetic record (SNR = -7 dB) . (e) The automatic picking result of the three algorithms for WGN noisy synthetic record (SNR = -10 dB). (f) Zoomed version of (d). (g) Zoomed version of (e).

For the detailed comparisons, the 45th to 70th sampling points in Figs. 8(d) and 8(e) are enlarged to obtain the Fig. 8(f) and 8(g), respectively. We can discover that the SPE algorithm's picking results of three components in one group (1st, 2nd and 3rd traces are one group, 4th , 5th and 6th traces are one group, and so on) are same. However, sometimes, the conventional method's picking results of three components in one group are different, which does not match the facts. From what we have discussed above, the conclusion can be drawn that the accuracy of SPE algorithm is much higher than the conventional methods. Moreover, by processing the three components together, SPE algorithm can precisely pick the arrival time of X,Y components where energy of valid signals is weak.

Reliability for different levels of real noise

As for reliability of the tested algorithm for different noise, the type of noise is changed, Fig. 9(a) shows the noisy record with real noise (SNR = -7 dB) and Fig. 9(b) shows the noisy record with real noise (SNR = -10dB). From Figs. 9(a) and 9(b), it is obvious that whether SNR = -7 dB or -10 dB, the valid signals are overwhelmed by the real noises, especially in horizontal components. In Figs. 9(c) and 9(d), time picks detected by the SPE algorithm, STA/LTA algorithm and the conventional polarization analysis method are marked by the symbols in green, black, pink, respectively. When SNR is -7dB, the picking results of SPE algorithm are accurate in all traces, but the picking results of STA/LTA algorithm are wrong in traces 3,5,6,7,8,9,12,14,15,18 and the picking results of the conventional polarization analysis method are wrong in traces 3,9,11,12,17,18. When SNR is -10 dB, the picking results of SPE algorithm are also accurate in all traces, but the picking results of STA/LTA algorithm are wrong in traces 1,2,3,5,6,9,10,12,15,16,18 and the picking results of the conventional polarization analysis method are wrong in traces 6, 9,14,15,17,18. From the data above, we can discover that the conventional methods often pick the arrival time mistakenly in horizontal components where the energy of valid signals is weak. However, the picking results of SPE algorithm are accurate in all traces. For a detailed comparison, the 45th to 70th sampling points in Figs. 9(c) and 9(d) are enlarged to obtain the Figs. 9(e) and 9(f), respectively. Similar to WGN, the conventional method's picking results of three components in one group are different. As stated above, the conclusion can be drawn that the SPE algorithm can adapt to low-SNR noise and have higher accuracy of picking. Also, it can precisely pick the arrival time of horizontal components.

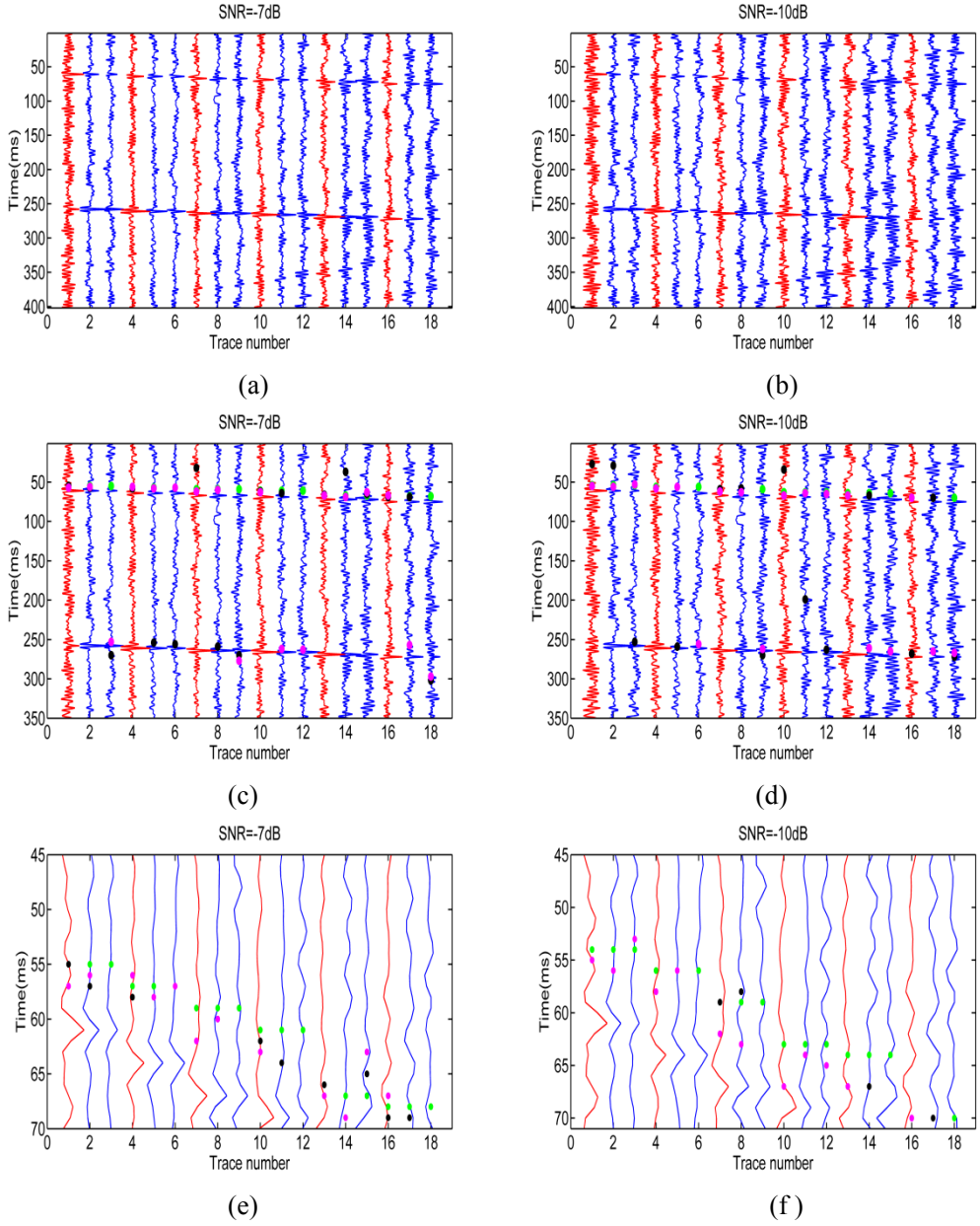

Fig. 9. First arrival times picked by three algorithms with real noises. (a) and (b) are noisy synthetic record with -7 dB and -10 dB， respectively. (c) Automatic picking results of three algorithms for real noises (SNR = -7 dB). (d) Automatic picking results of the three algorithms for real noises (SNR = -10 dB). (e) The enlarged view of (b). (f) The enlarged view of (d).

TESTS WITH FIELD MICROSEISMIC DATA

Then, the SPE algorithm is validated by 15-channel hydraulic fracturing data acquired in an oil field of China shown in Fig. 10(a). The observation well is located in 300 m from the treatment well. The sampling rate is 0.001s. The vertical components (Z component) are shown in red and the horizontal components(Y,X components) in blue. The arrival times are picked by applying the SPE algorithm, STA/LTA algorithm and the conventional polarization analysis method. In Fig. 10(b), the picking results of SPE

algorithm, the conventional polarization analysis method and STA/LTA algorithm are marked in green, pink, black dots. We enlarged Fig. 10(b) to get Fig. 10(c). In order to compare the three methods minutely, the detailed picking results are listed in Table–VII, the red numbers represent the false picking. The picking results of SPE algorithm are accurate in all traces, but the picking results of STA/LTA algorithm are wrong in traces 2,3,5,9,10,12,14,15 and the picking results of the conventional polarization analysis method are wrong in traces 3,9,10,12,14,15. Similar to Synthetic microseismic data, the false picking often appears in horizontal components (Y,X components) by conventional methods. So SPE algorithm is superior to conventional methods when processing the low-SNR field microseismic data.

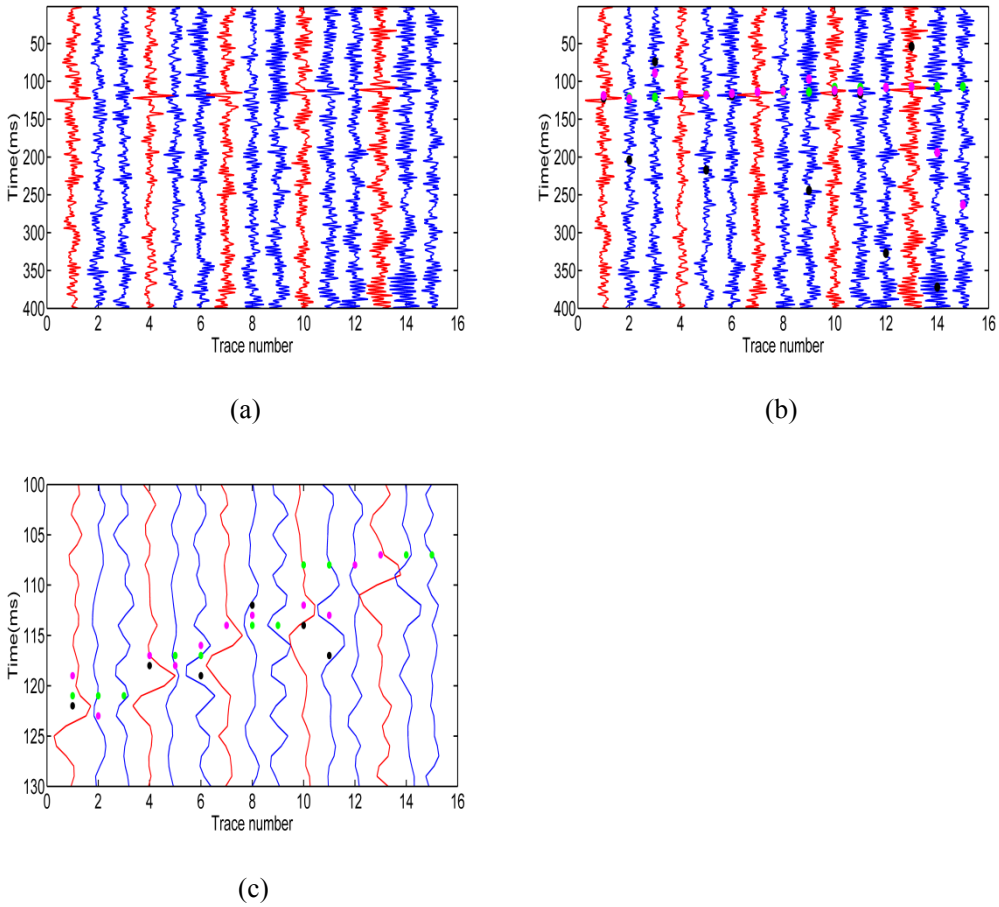

Fig. 10. (a) Real field miscroseismic record. (b) The automatic picking results of the three algorithms for real field miscroseismic record. (c) Zoomed version of (b).

Table VII. Time picking results of the three algorithm in field microseismic record.

Trace number	1	2	3	4	5	6	7	8	9	10	11	12	13	14	15
SPE algorithm (ms)	121	121	121	117	117	117	114	114	114	108	108	108	107	107	107
STA/LTA algorithm (ms)	122	204	74	118	217	119	114	112	224	117	112	327	109	54	372
The conventional analysis method(ms)	119	123	89	117	118	116	114	113	97	116	113	108	107	194	263
The correct arrival time（ms）	120	120	120	117	117	117	113	113	113	110	110	110	106	106	106

CONCLUSION

The SPE algorithm proposed in this paper mainly bases on the Shearlet transform, polarization analysis method and 3D weighted entropy ratio. By using the multi-scale and multi-direction features of Shearlet transform, the valid signals are highlighted. Furthermore, the polarization analysis method and the 3D weighted entropy ratio algorithm are proposed to process the three components of Shearlet coefficients together. This can overcome the conventional methods' shortcoming - the picking results of three components in one group are different and the false pickings often appear in horizontal components (Y,X components). In the 3D weighted entropy ratio algorithm, the weight factor is proposed to reflect the change of frequency and energy. Also, the entropy is introduced to highlight the valid signals. The SPE algorithm is tested on synthetic microseismic data. The results show that the accuracy of SPE algorithm is still up to 90% when the SNR is as low as -10dB. Also, the accuracy of SPE algorithm is still higher than 50% when the SNR is as low as -17dB, as shown in Table VIII. This ability of resisting noises can definitely meet the requirements of microseismic date processing. Also the comparison with conventional algorithms shows the better performance of SPE algorithm, especially in the horizontal components (Y,X components). From the experimental data, we can see that SPE algorithm can pick arrival times much more accurately than the other two methods at low SNRs. So compared conventional method, the SPE algorithm is much more suitable for microseismic signal processing.

Table VIII. Time picking results of SPE algorithm in lower SNRs.

The WGN tests						
SNR(dB)	numbers of signals	accurate picking	inaccurate picking	Signals picking within 0.002s	Signals picking within 0.001s	Signals picking without errors
-17	1000	508	492	360	264	178
-18	1000	488	512	345	256	152

REFERENCES

Allen, R.V., 1978. Automatic earthquake recognition and timing from single traces. Bull. Seismol. Soc. Am., 68: 1521-1532.

Allen, R.V., 1982. Automatic phase pickers: Their present use and future prospects. Bull. Seismol. Soc. Am., 72: 146-156.

Deflandre, J.P. and Dubesset, M., 1992. Identification of P/S wave successions for application in microseismicity. Pure Appl. Geophys., 139: 405-420. doi: 10. 1007/BF00879944.

Guo, K. and Labate, D, 2007. Optimally sparse multidimensional representation using shearlets. SIAM J. Math., Anal., 39: 298-318.

Houska, R. and William, J.C., 2007. The nonexistence of Shearlet scaling function. Appl. Comput. Harmon. Anal., 32: 298-318.

Kutyniok, G. and Labate, D., 2007. Construction of regular and irregular shearlets. Wave Theory Appl., 1: 1-10.

Kutyniok, G. and Lim, W.Q., 2011. Compactly supported Shearlets are optimally sparse. J. Approx. Theory, 163: 1564-1589.

Leonard, M. and Kennett, B.L.N., 1999. Muli-component antoregressive techniques for analysis of seismograms. Phys. Earth Planet. Inter., 113: 247-263.

Rodriguez, I.V., Bonar, D. and Sacchi, M., 2011. Microseismic data denoising using a 3C group sparsity constrained time-frequency transform. Geophysics, 77(2): V21-V29.

Saragiotis, C.D., Hadjileontiadis, L.J. and Panas, S.M., 2002. PAI-S/K: A robust automatic seismic P-phase arrival identification scheme. IEEE Transact. Geosci. Remote Sens., 40: 1395-1404.

Stevenson, R., 1976. Automatic earthquake recognition and timing from single trace. Bull. Seismol. Soc. Am., 68: 1521-1532.

Tetsuo, T. and Kitagawa, G., 1991. Estimation of arrival of seismic waves by multivariate time series model. Ann. I. Stat. Math., 43: 407-433.

Warpinski, N., 2009. Micreseismic monitoring: Inside and out. J. Petrol. Technol., 61(11): 80-85.

Yi, S., Labate, D., Easley, G.R. and Krim, H.A., 2009. Shearlet approach to edge analysis and detection. IEEE Transact. Image Process., 18: 929-941.

Zhao, H., Li, Y. and Zhang, C., 2016. SNR enhancement for downhole microseismic data using CSST. IEEE Geophys.. Remote Sens. Lett., 13: 1139-1143.